Calculated electronic structure of Au_{13} clusters

Ramiro Arratia-Perez, Agustin F. Ramos, and G. L. Malli
Department of Chemistry and Theoretical Sciences Institute, Simon Fraser University, Burnaby, British Columbia, Canada V5A 1S6
(Received 16 August 1988)

The electronic structure of cubo-octahedral and icosahedral Au_{13} clusters has been investigated by the self-consistent-field molecular-orbital Dirac scattered-wave method. Double-point-group–symmetry considerations indicate that the icosahedral cluster will undergo static Jahn-Teller distortion, while the cubo-octahedral cluster cannot distort because of a Kramers degeneracy in the ground state. Molecular Zeeman and hyperfine interactions are calculated for the cubo-octahedral Au_{13} cluster through a first-order perturbation to the Dirac Hamiltonian. The predicted g tensors and ^{197}Au hyperfine tensors are consistent with a nearly isotropic paramagnetic-resonance spectrum. The calculated density-of-states (DOS) curves for the Au_{13} clusters show similar features to those obtained in photoemission experiments of small clusters of gold. Relativistic effects increase the d-band width by more than 1 eV, and spin-orbit interaction splits the occupied d band by about 2 eV in both clusters. These calculated values are approximately 75% of the observed values for gold in the bulk metal. It is clearly shown that the overlap of the d band by the s-p band is mainly due to relativistic effects.

INTRODUCTION

The electronic structure, optical, magnetic, and structural properties of small metallic clusters is a subject of extensive experimental and theoretical research at present because of its relevance to surface phenomena, growth morphology, heterogeneous catalysis, and materials science and technology.[1–7] In particular, the structural properties of small bare clusters of gold have been studied by transmission electron microscopy (TEM),[8–11] scanning tunneling microscopy (STM),[12] and high-resolution electron microscopy (HREM).[13,14] These studies have indicated that small gold particles are consistent with both cubo-octahedral (O_h) and icosahedral (I_h) geometries.[8–14] The evolution of band structure in gold clusters has been investigated by photoemission spectroscopy.[15–18] Ligand-free gold cationic clusters can be generated by laser vaporization techniques and selected by mass spectrometry,[19,20] whereas the synthesis of the icosahedral[21] $[Au_{13}L_{10}Cl_2]^{3+}$ and cubo-octahedral[22] $Au_{55}L_{12}Cl_6$ gold clusters (where L is a triarylphosphine ligand), were reported a few years ago.

Despite the large volume of experimental data available for gold clusters only few first-principles fully relativistic molecular-orbital calculations have been reported for gold clusters.[23–25] Recently we generated for the first time the symmetry-adapted basis functions for the icosahedral double-point group (I_h^*) enabling us to calculate the relativistic molecular orbitals (MO's) for the icosahedral Au_{13} cluster.[23] In the above mentioned studies,[23–25] we have shown that the nonrelativistic description of chemical bonding for these heavy atom systems is unrealistic, since, due to relativistic effects there is significant "s-d" hybridization in the bonding molecular orbitals.

In this study we have calculated the relativistic molecular orbitals for the cubo-octahedral Au_{13} cluster via the self-consistent-field (SCF) Dirac scattered-wave (DSW) method. An analysis of the valence band of both the icosahedral[23] and cubo-octahedral Au_{13} clusters is presented, and our results are compared with the photoemission[15–18] results obtained for gold clusters. The calculated relativistic (DSW) density-of-states (DOS) curves show features similar to those obtained in photoemission experiments. The calculated d-band width and d-band splitting are in good agreement with the experimentally reported values. It is shown that the overlap of the d band by the s-p band is mainly a relativistic effect. We also report nonrelativistic-limit (NR) calculations for both the clusters in order to ascertain the importance of relativistic effects on these heavy atom systems. Our results show that the nonrelativistic-DOS curves differ significantly from those obtained experimentally.

CALCULATIONS

The Dirac scattered-wave (DSW) method was developed by Yang and co-workers,[26–29] and except for the change of boundary conditions it is analogous to the relativistic Korringa-Kohn-Rostoker (RKKR) energy band-structure technique for solids.[30] The DSW methodology uses the Dirac equation rather than the Schrödinger equation to generate the one-electron orbitals, and thus implicitly includes the relativistic effects such as spin-orbit interaction, Darwin and mass-velocity corrections. The molecular spinors as well as the overall electronic four-component wave functions transform according to the double point group of the molecular system under investigation.[26–29]

Our method for calculating the molecular g tensors and hyperfine interactions has been described earlier.[31] It is based upon a first-order perturbation to the Dirac Hamiltonian so that the effects of magnetic fields are described by the operator H_1,

$$H_1 = e\boldsymbol{\alpha}\cdot\mathbf{A}\ , \tag{1}$$

where $\boldsymbol{\alpha}$ is the vector of 4×4 Dirac matrices and $\mathbf{A}$ is the electromagnetic vector potential. For the Zeeman interaction $\mathbf{A}=\frac{1}{2}(\mathbf{B}\times\mathbf{r})$, where $\mathbf{B}$ is the external magnetic field. For the hyperfine interaction $\mathbf{A}=(\mu\times\mathbf{r})/r^3$, where μ is the nuclear magnetic moment. Matrix elements of these operators are evaluated in the basis spanning the two rows of the E_{3g} representation (of the O_h^* group) of the partially occupied relativistic molecular orbital. The resulting perturbation energies are then fitted to the usual spin Hamiltonian (H_{spin})

$$H_{\text{spin}}=\mathbf{S}'\cdot g\cdot\mathbf{B}+\mathbf{S}\cdot A_n\cdot\mathbf{I}_n\ , \tag{2}$$

where a value of $S'=\frac{1}{2}$ is used to describe the ground-state Kramers doublet, $\mathbf{I}_n$ is the nuclear-spin operator, and n indicates the central or the peripheral gold nucleus.

The Au-Au distances for the cubo-octahedral cluster were taken to be equal to the nearest-neighbor distances in crystalline gold (2.88 Å). It has been observed that noble-metal particles of around 13 atoms show a small contraction of the nearest-neighbor distance compared to that of the bulk metal.[32] The nonrelativistic (NR) limits of the calculations were obtained with a large value of the velocity of light in the DSW calculations. The coordinate system for the cubo-octahedral (O_h) and icosahedral (I_h) geometries of the Au_{13} clusters are given in Fig. 1.[33] These all-electron fully relativistic molecular-orbital calculations are the first to be reported for any cluster of this size in different geometries.

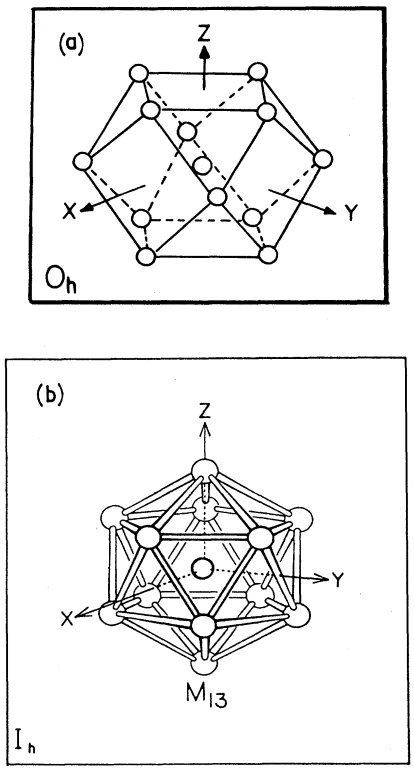

FIG. 1. The cubo-octahedral (a) and icosahedral (b) Au_{13} clusters (they have a diameter of about 5 Å).

RESULTS AND DISCUSSION

The calculated nonrelativistic (NR) limit and relativistic (DSW) valence-orbital energies and their corresponding symmetries for the icosahedral and cubo-octahedral Au_{13} clusters are shown in Fig. 2. Omitting the g or u subscript for parity, the I_h point group has the single-valued irreducible representations (irreps) denoted here by $A(1)$, $T_1(3)$, $T_2(3)$, $G(4)$, and $H(5)$ (where the number of parentheses indicates its dimension), and the double-valued irreps $E_2(2)$, $E_3(2)$, $Q(4)$, and $I(6)$. In contrast, the O_h point group has the single-valued irreps $A_1(1)$, $A_2(1)$, $E(2)$, $T_1(3)$, and $T_2(3)$, and the double-valued irreps $E_2(2)$, $E_3(2)$, and $Q(4)$. An analysis of the descent in symmetry from the full rotation group to the I_h and O_h point groups shows that the I_h irreps G, H, and I correlate with the direct sum of the O_h irreps $A_{1(2)}+T_{1(2)}$, $E+T_{1(2)}$, and $E_{2(3)}+Q$, respectively. Furthermore, the spin-orbit splitting correlations for each point group indicates that for I_h the irreps T_1, G,

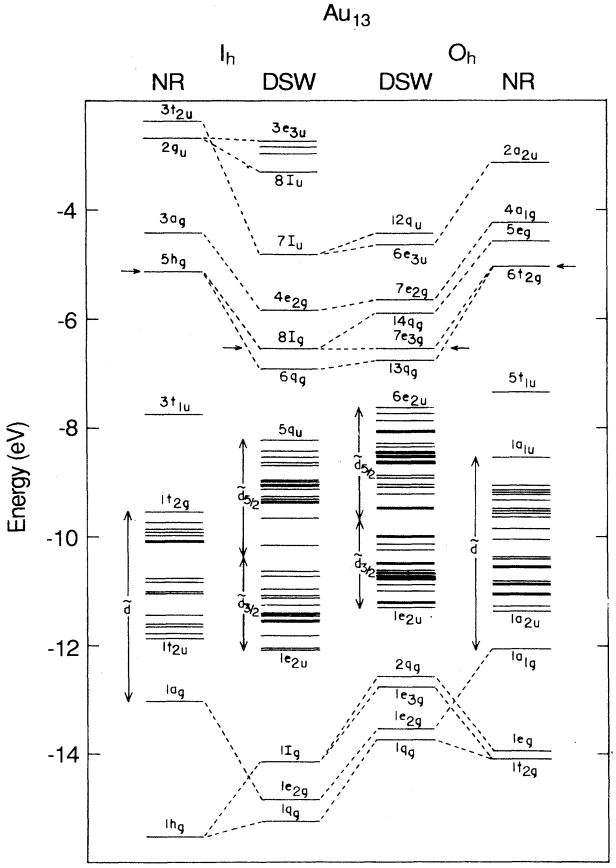

FIG. 2. Nonrelativistic (NR) limit and relativistic (DSW) valence energy levels of the icosahedral (I_h) and cubo-octahedral (O_h) Au_{13} cluster, and their corresponding orbital symmetry. The Fermi level is indicated by an arrow in each case.

and H split into E_2+Q, E_3+I, and $Q+I$; and in the O_h point group the T_1 and T_2 irreps split into E_2+Q, and E_3+Q, respectively. These splittings and group correlations are indicated by dashed lines in Fig. 2 for some of the lowest- and highest-lying molecular orbitals (MO's). In particular, there is a dispersion of levels around the Fermi levels (indicated by an arrow in Fig. 2) due to the change in crystal-field symmetry on going from icosahedral to cubo-octahedral geometry.

The nonrelativistic-limit (NR) calculations for the cubo-octahedral (O_h) cluster predict $^2T_{2g}$ as its ground state arising from the electronic configuration t_{2g}^5. This is in agreement with the nonrelativistic *ab initio* self-consistent-field (SCF)- linear combination of atomic orbitals (LCAO),[34(a)] $X\alpha$–discrete-variational (DV),[34(b)] and $X\alpha$–scattered-wave (SW) [Ref. 34(c)] calculations on the corresponding Cu_{13} cluster. However, the nonrelativistic ground state for the icosahedral (I_h) gold cluster was predicted to be ^6A_g arising from the h_g^5 electronic configuration,[23] in accord with the *ab initio* LCAO calculation[34(a)] on the icosahedral Cu_{13} cluster. The charge breakdown of the nonrelativistic highest occupied molecular orbital (HOMO) or Fermi (E_F) level for both the gold clusters indicates that these are antibonding combinations with mainly 6*s*-6*p* character (60% 6*s* and 32% 6*p* in the O_h cluster, and 51% 6*s* and 43% 6*p* in the I_h cluster). The calculated nonrelativistic *d*-bandwidth is larger for the O_h gold cluster (2.84 eV) than for the icosahedral cluster (2.28 eV). A similar conclusion has also been reached for the I_h and O_h Cu_{13} clusters from an *ab initio* SCF-LCAO calculation.[34(a)]

The relativistic descriptions of both the gold clusters differ significantly from the corresponding nonrelativistic description presented above. The relativistic highest occupied molecular orbitals (HOMO's) or Fermi levels split due to spin-orbit interaction by 0.25 and 0.41 eV in the O_h and I_h gold clusters, respectively. Due to spin-orbit interaction the nonrelativistic ^6A_g ground state of the I_h cluster becomes a doublet of a sixfold orbital (I_g). The immediate consequence of this effect is that the relativistic formalism indicates that the icosahedral Au_{13} cluster should show a weak paramagnetic susceptibility, in contrast to the nonrelativistic description which predicts a much stronger paramagnetic behavior.[23] The nonrelativistic $^2T_{2g}$ ground state of the O_h gold cluster splits due to spin-orbit interaction into the electronic states of twofold (E_{3g}) and fourfold (Q_g) symmetries. Thus, the relativistic ground state of the cubo-octahedral cluster corresponds to a Kramers doublet of E_{3g} symmetry and should exhibit a characteristic paramagnetic resonance spectrum.

It is interesting to note that from considerations of double group theory the icosahedral Au_{13} cluster will undergo static Jahn-Teller[35] distortion due to orbital degeneracy in its ground state (the unpaired electron is located in the sixfold orbital), whereas the cubo-octahedral Au_{13} cluster (because there is no orbital degeneracy in its ground state) would not distort, since the twofold spin degeneracy (Kramers) cannot produce any instability of the molecular configuration.[35] These arguments are in agreement with the recent extended x-ray-absorption fine-structure (EXAFS) studies on Cu and Ag microclusters isolated in an argon matrix which provided evidence for the existence of face-centered-cubic (O_h) structures of about 13 atoms.[32,36] We have also calculated the first ionization potentials (IP) via the transition state method for both the clusters. The predicted first IP's are 8.35 and 8.43 eV for the cubo-octahedral and icosahedral Au_{13} clusters, respectively.

The results of the calculated electron spin-resonance parameters for the cubo-octahedral Au_{13} cluster are given in Table I. For the molecular Zeeman interaction, the calculation predicts an isotropic *g* tensor with a value of 1.9114. In the absence of spin-orbit mixing, the Au_{13} cluster will exhibit resonances at the spin-only value of 2.0023. A similar negative *g* shift has been observed in the paramagnetic resonance spectrum of matrix isolated Au_3 cluster.[37]

For the ^{197}Au hyperfine interactions, Table I shows that the calculation predicts a small negative isotropic hyperfine tensor for the central gold atom. This small contribution comes mostly from the "orbital term" which arises from unquenched orbital angular momentum, since the Fermi contact contributions vanish by symmetry and the spin-dipolar interactions (arising from the $d_{5/2}$ spinors) are almost negligible. Results for the peripheral gold atom hyperfine interactions are also given in Table I. These are predicted to be nearly isotropic; the small anisotropic character of the hyperfine tensor could be attributed to the amount of the $6p_{3/2}$, $5d_{3/2}$, and $5d_{5/2}$ spinors mixed into the partially occupied molecular orbital ($7e_{3g}$) which has about 60% $6s_{1/2}$ character. Thus, our symmetry analysis and the calculated values of the magnetic resonance parameters of the Au_{13} clusters clearly suggest that a low temperature paramagnetic resonance experiment should be able to distinguish between the cubo-octahedral and icosahedral geometrical arrangements and that the spectrum should be nearly isotropic. It is worth noting, that the matrix isolated Au_3 cluster also shows a largely isotropic paramagnetic resonance spectrum.[37]

The molecular-orbital representation of the electronic wave functions and the use of double group orbital symmetries allow us to distinguish between "surface orbitals" (with no components on the central atom) and "bulk orbitals" (which have contributions from all the 13 atoms).[34(c)] Thus, both clusters have a total of 143 valence electrons of which 80% correspond to bulk orbitals in the cubo-octahedral cluster, while only 62% of the valence electrons correspond to bulk orbitals in the icosahedral cluster. Consequently, the icosahedral clus-

TABLE I. Calculated magnetic resonance parameters of the cubo-octahedral Au_{13} cluster.

Molecular *g* tensor	1.9114	
Hyperfine tensors (MHz)		
^{197}Au central	-9	
^{197}Au peripheral	$A_\parallel$	$A_\perp$
	187	190

ter has more surface electrons which is consistent with the larger number of nearest-neighbor interactions (42 versus 36), and therefore would exhibit a larger d-band width than the O_h cluster. This is in agreement with the present relativistic calculations.

A direct comparison with the photoemission measurements[15–18] can be made through the density of states (DOS) curves, d-band width and the spin-orbit splitting of the d band. Figures 3(c) and 3(d) compare the DOS curves (Gaussian-broadened discrete levels with a broadening parameter of 0.6 eV) for the cubo-octahedral and icosahedral Au_{13} clusters as calculated by the DSW and its nonrelativistic (NR) limit calculations. Significant differences are noticeable. The NR-DOS curves for both the gold clusters [Figs. 3(c) and 3(d)] show essentially three peaks. The small peak at higher energy (which contains the E_F level) corresponds mainly to the occupied s-p band. The higher intensity peak corresponds to the main d band, while the low-energy peak is due to the discrete nature of the central gold atom curves. The nonrelativistic E_F level for both the clusters is completely embedded in the s-p band and is quite well separated from the main d band.

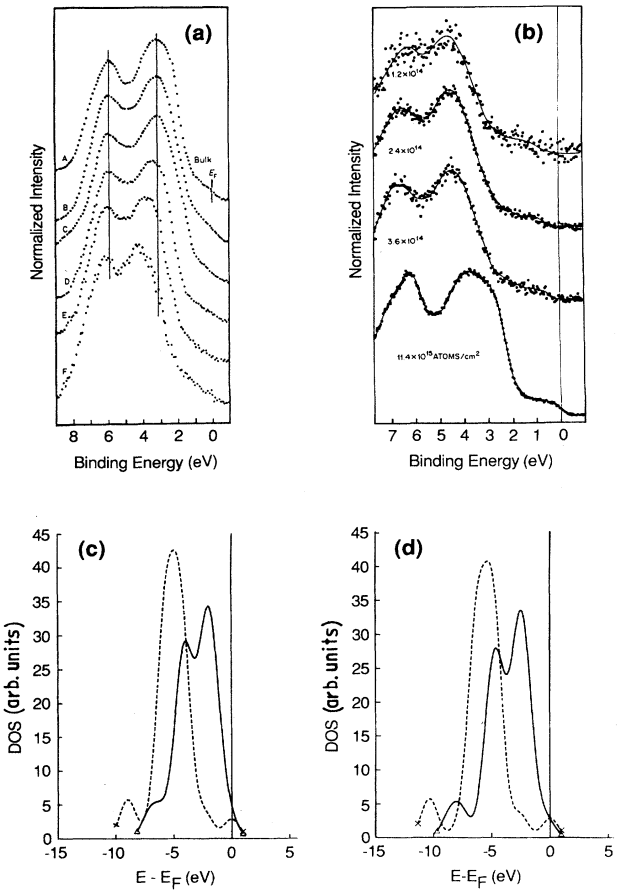

FIG. 3. Valence-band photoemission spectra of various coverages of gold clusters on different substrates, (a) and (b), and calculated valence density-of-states (DOS) curves of Au_{13} clusters, (c) and (d). (a) Photoemission spectra of gold bulk metal (curve A), and various coverages of gold on NaCl substrate (curves B–F). The lowest coverage (1.0×10^{15} atoms/cm^2, curve F) corresponds to gold cluster sizes of about 15 Å diameter (Ref. 16). (b) Photoemission spectra of various coverages of gold on a vitrous carbon substrate (Ref. 18). The substrate's contribution to each spectrum has been subtracted. (c) Nonrelativistic limit (dashed line) and relativistic (solid line) Gaussian-broadened DOS of the cubo-octahedral Au_{13} cluster. (d) Nonrelativistic limit (dashed line) and relativistic (solid line) DOS of the icosahedral Au_{13} cluster. The energies are shifted in each case so that the Fermi level (E_F) is at 0 eV.

The relativistic DSW-DOS curves for both the clusters (Fig. 3) show essentially three main peaks, and it is evident that the s-p band completely overlaps the d band in both the clusters. However, there is a difference in these DOS curves at the Fermi level, since the curve corresponding to the cubo-octahedral cluster shows a larger density of states than the icosahedral cluster (see Fig. 3). The overlap of the d band by the s-p band arises due to relativistic effects since the d band is destabilized (indirect effect) and the s-p band is stabilized (direct effect).[24] Furthermore, the charge breakdown of the relativistic E_F level for both clusters indicates that the amount of d character is larger in the O_h cluster than the I_h cluster (26% versus 16%). The two main peaks in each cluster are attributed to the spin-orbit coupling effect, and the drop in intensity of the DSW-DOS curves can be assigned to the enhanced s-d hybridization in their valence band.

The x-ray-photoemission spectra (XPS) of the valence band of isolated gold clusters can be obtained after subtraction of the substrate spectrum[16,18] and are presented in Fig. 3. It is clear that there is a close correspondence between the relativistic (DSW) DOS curves and those obtained experimentally, while the nonrelativistic (NR) DOS curves differ significantly from the experimental curves. The calculated relativistic d-band widths are 3.74 and 3.92 eV for the O_h and I_h clusters, respectively, while the calculated splitting of the d band for the O_h and I_h clusters are 2.1 and 2.2 eV. These calculated values are in fairly good agreement with the experimental values obtained from the photoemission spectra of the valence band of gold clusters.[15–18] However, the observed d-band width and d-band splitting in crystalline gold are 5.24 and 2.80 eV, respectively.[16,38] Thus, the calculated d-band width and d-band splitting of the Au_{13} clusters are approximately 75% of the observed values in the bulk metal, indicating that the onset of the metallic state is noticeable even for clusters of this size.

CONCLUSIONS

To summarize, we have presented the first fully relativistic molecular orbital calculations for Au_{13} clusters and have obtained information which could be useful for the experimental study of very small gold particles. It has been shown that nonrelativistic cluster calculations on heavy-atom systems may lead to an unrealistic description of their electronic structure since relativistic effects are very large for such systems. In the clusters studied here, relativistic effects increase the d-band width by more than 1 eV, split the d band by about 2 eV, and induce an effective overlap of the d band with the s-p band.

Furthermore, double-point-group–symmetry arguments indicate that the icosahedral geometry of Au_{13} will undergo static Jahn-Teller distortion, while the cubo-octahedral cluster will not distort due to a Kramers degeneracy in the ground state. The predicted magnetic properties for the cubo-octahedral Au_{13} cluster are consistent with an isotropic paramagnetic resonance spectrum. It is also clear from this study that although the onset of the metallic state is discernible in the Au_{13} clusters, a cluster with a larger number of gold atoms would be required to mimic completely the band structure of bulk metallic gold.

ACKNOWLEDGMENT

This work was supported in part by the Natural Sciences and Engineering Research Council (NSERC) of Canada through Grant No. A3598.

[1]Proceedings of a Symposium on Small Particles and Inorganic Clusters, Berlin, 1984 [Surf. Sci. **156**, 3 (1985)].

[2]W. Jr. Weltner and R. J. Van Zee, Annu. Rev. Phys. Chem. **35**, 291 (1984).

[3]J. Koutecky and P. Fantucci, Chem. Rev. **86**, 539 (1986).

[4]W. Jr. Weltner and R. J. Van Zee, in *Comparisons of Ab Initio Quantum Chemistry with Experiment for Small Molecules,* edited by R. J. Bartlett (Reidel, Dordrecht, 1985).

[5]M. D. Morse, Chem. Rev. **86**, 1049 (1987).

[6]S. Iijima, in *Microclusters,* edited by S. Sugano, V. Nishina, and S. Ohnishi (Springer-Verlag, Berlin, 1987).

[7]J. A. Howard and B. Mile, Accts. Chem. Res. **20**, 173 (1986).

[8]S. Ogawa and J. Ino, J. Cryst. Growth **13**, 48 (1972).

[9]C. Solliard, Ph. Buffat, and F. Faes, J. Cryst. Growth **32**, 123 (1976).

[10]C. Y. Yang, K. Heineman, M. J. Yacaman, and H. Poppa, Thin Solid Films **58**, 163 (1979).

[11]L. D. Marks and D. J. Smith, J. Cryst. Growth **54**, 425 (1981).

[12]D. W. Abraham, K. Sattler, E. Ganz, H. Mamim, R. E. Thomson, and J. Clarke, Appl. Phys. Lett. **49**, 853 (1986).

[13]S. Iijima and T. Ichihashi, Japan. J. Appl. Phys. **24**, L125 (1985); **23**, L347 (1984).

[14]S. Iijima and T. Ichihashi, Phys. Rev. Lett. **56**, 616 (1986).

[15]K. S. Liang, W. R. Salaneck, and I. A. Aksay, Solid State Commun. **19**, 329 (1976).

[16]H. Roulet, J. M. Mariot, G. Dufour, and C. F. Hague, J. Phys. F **10**, 1025 (1980).

[17]S. T. Lee, G. Apai, M. G. Mason, R. Benbow, and Z. Hurych, Phys. Rev. B **23**, 505 (1981).

[18]G. K. Wertheim, S. B. DiCenzo, and S. E. Youngquist, Phys. Rev. Lett. **51**, 2310 (1983).

[19]P. Sudraud, C. Colliex, and J. Van de Walle, J. Phys. (Paris) **40**, L207 (1979).

[20]A. R. Waugh, J. Phys. D **13**, L203 (1980).

[21]C. E. Briant, B. C. Theobald, J. W. White, L. K. Bell, and D. M. P. Mingos, J. Chem. Soc. Chem. Commun. 201 (1981).

[22]G. Schmid, Struct. Bond. **62**, 51 (1985).

[23]A. F. Ramos, R. Arratia-Perez, and G. L. Malli, Phys. Rev. B Condens. Matter **35**, 3790 (1987).

[24]R. Arratia-Perez and G. L. Malli, J. Chem. Phys. **84**, 5891 (1986).

[25]R. Arratia-Perez and G. L. Malli, Chem. Phys. Lett. **125**, 143 (1986).

[26]C. Y. Yang and S. Rabii, Phys. Rev. A **12**, 362 (1975).

[27]C. Y. Yang, in *Relativistic Effects in Atoms, Molecules and Solids,* edited by G. L. Malli (Plenum, New York, 1983).

[28]C. Y. Yang and D. A. Case, in *Local Density Approximations in Quantum Chemistry and Solid State Physics,* edited by J. Dahl and J. P. Avery (Plenum, New York, 1984).

[29]D. A. Case and C. Y. Yang, J. Chem. Phys. **72**, 3443 (1980).

[30](a) Y. Onodera and M. Okazaki, J. Phys. Soc. Jpn. **21**, 1273 (1966). (b) S. Takada, Progr. Theor. Phys. **36**, 224 (1966).

[31](a) R. Arratia-Perez and D. A. Case, J. Chem. Phys. **79**, 4939 (1983). (b) R. Arratia-Perez and G. L. Malli, J. Chem. Phys. **85**, 6610 (1986). (c) R. Arratia-Perez and D. S. Marynick, Phys. Rev. B **37**, 4893 (1988).

[32]P. A. Montano, G. K. Shenoy, E. E. Alp, W. Schulze, and J. Urban, Phys. Rev. Lett. **56**, 2076 (1986).

[33]The cubo-octahedral geometry is the structure corresponding to the local arrangement of atoms in the face-centered-cubic (fcc) crystalline gold, while the icosahedral geometry characterized by a fivefold rotational symmetry axis is incompatible with translational symmetry.

[34](a) J. Demuynck, M. M. Rohmer, A. Strich, and A. Veillard, J. Chem. Phys. **75**, 3443 (1981); (b) B. Delley, D. E. Ellis, A. J. Freeman, E. J. Baerends, and D. Post, Phys. Rev. B **27**, 2132 (1983); (c) R. P. Messmer, S. K. Knudson, K. H. Johnson, J. B. Diamond, and C. Y. Yang, Phys. Rev. B **13**, 1396 (1976).

[35](a) H. A. Jahn and E. Teller, Proc. R. Soc. London, Ser. A **161**, 220 (1937); (b) H. A. Jahn, Proc. R. Soc., London Ser. A **164**, 117 (1938).

[36]P. A. Montano, W. Schulze, B. Tesche, G. K. Shenoy, and T. I. Morrison, Phys. Rev. B **30**, 672 (1984).

[37]J. A. Howard, R. Sutcliffe, and B. Mile, J. Chem. Soc. Chem. Commun. 1449 (1983).

[38]Extensive comparisons of DOS curves obtained from relativistic energy-band structure calculations and photoemission experiments on crystalline gold are given in D. A. Shirley, Phys. Rev. B **5**, 4709 (1972).